Applied Catalysis B: Environmental 172–173 (2015) 154–164

Contents lists available at ScienceDirect

Applied Catalysis B: Environmental

journal homepage: www.elsevier.com/locate/apcatb

# Maximizing carbon efficiency of petrochemical production from catalytic co-pyrolysis of biomass and plastics using gallium-containing MFI zeolites

Jian Li, Yanqing Yu, Xiangyu Li, Wei Wang, Gang Yu, Shubo Deng, Jun Huang, Bin Wang, Yujue Wang*

*School of Environment, Beijing Key Laboratory for Emerging Organic Contaminants Control, State Key Joint Laboratory of Environmental Simulation and Pollution Control, Tsinghua University, Beijing 100084, China*

ARTICLE INFO

*Article history:*
Received 14 November 2014
Received in revised form 18 January 2015
Accepted 14 February 2015
Available online 17 February 2015

*Keywords:*
Aromatic hydrocarbon
Olefin
Xylene
Gallium
ZSM-5

ABSTRACT

A series of gallium-containing MFI zeolites were prepared via impregnation of conventional aluminosilicate ZSM-5 with Ga (Ga/ZSM-5) or hydrothermal synthesis of galloaluminosilicate (Ga–Al–Si) and gallosilicate (Ga–Si) MFI zeolites. These Ga-containing zeolites were then tested as the catalysts for co-feed catalytic fast pyrolysis (CFP) of pine wood and low-density polyethylene (LDPE) mixtures. Compared with conventional ZSM-5 zeolites, the Ga-containing MFI zeolites considerably increased the yields of valuable petrochemicals (monoaromatic hydrocarbons and olefins) and decreased the yields of undesired polyaromatic hydrocarbons and low-value alkanes from the co-feed CFP. In addition, Ga–Al–Si and Ga–Si zeolites generally produced both higher yields and selectivities for valuable petrochemicals (e.g., *p*-xylene and olefins) than Ga/ZSM-5 in the co-feed CFP. The results indicate that Ga-containing zeolites may be used to improve petrochemical production in co-feed CFP of biomass and plastics, and direct hydrothermal synthesis of Ga–Al–Si and Ga–Si MFI zeolites may provide a more convenient and better alternative to post modification of ZSM-5 with Ga to prepare Ga-containing zeolites for co-feed CFP.



## 1. Introduction

Aromatic hydrocarbons and olefins are the building-blocks of the petrochemical industry and widely used to manufacture numerous useful products, such as plastics, synthetic rubbers, solvents, and pharmaceuticals. Due to their extensive applications, the market demand for aromatics and olefins is increasing rapidly worldwide [1–3]. However, the petroleum reserves on the earth, which are the conventional source for producing aromatics and olefins, are depleting at a rapid rate. This dilemma has stimulated ever-increasing interest in seeking alternative feedstocks (especially renewable sources) for producing aromatics and olefins [4–6].

Biomass and plastic wastes have been considered attractive feedstocks for producing renewable petrochemicals due to their low cost and abundance [4,7,8]. Each year, tremendous amounts of biomass and plastic wastes (e.g., corn stover, papers, and plastic films) are generated globally from municipal, industrial, and agricultural sources [4,8,9]. These wastes contain considerable carbon and hydrogen contents that can be used to produce hydrocarbon petrochemicals. Therefore, many conversion technologies have been developed with the aim of producing renewable petrochemicals from biomass and plastic wastes [4,6,8]. Among them, catalytic fast pyrolysis (CFP) has attracted growing attention, because it can rapidly convert solid biomass and plastic feedstocks directly into valuable aromatic and olefin products (e.g., benzene, toluene, xylenes (BTX), ethylene, and propylene) [6,7,10–12]. These aromatics and olefins can fit easily into the existing infrastructure of petrochemical industry. For example, BTX, ethylene, and propylene are five of the six most important primary petrochemicals that are extensively used in the petrochemical industry as feedstocks to make numerous petrochemical intermediates and commercial products [5,13].

CFP involves rapidly heating biomass or plastic feedstocks in the presence of catalysts (e.g., zeolites or metal oxides) [6,10,11,14]. During CFP, biomass and plastics undergo thermal and/or catalytic cracking to form volatile intermediates, which are then further catalytically converted over the catalysts to yield final products [12,15–21]. The whole conversion process can be completed in a single reactor at short reaction times (e.g., in seconds). Notably, although biomass (e.g., cellulose, hemicellulose, and lignin) and plastics (polyethylene (PE), polypropylene (PP), and polystyrene

* Corresponding author at: School of Environment, Tsinghua University, Beijing 100084, China. Tel.: +86 10 62772914; fax: +86 10 62785687.
*E-mail address:* wangyujue@tsinghua.edu.cn (Y. Wang).

http://dx.doi.org/10.1016/j.apcatb.2015.02.015
0926-3373/

(PS)) have very different chemical compositions and polymer structures, they can be converted to very similar aromatic and olefin products when they are catalytically pyrolyzed with ZSM-5 zeolites [9,12,16,20,22–25]. Furthermore, recent studies have shown that when biomass and plastics (e.g., cellulose and PE) are co-fed in CFP with ZSM-5, they can have a significant synergy enhancing aromatic production [9,12,22,23]. These results indicate that co-feeding of biomass with plastics has a beneficial effect on improving petrochemical production in CFP [9,12,22,23].

However, the results also show that the product distribution in co-feed CFP of biomass and plastic mixtures with ZSM-5 zeolites still has vast potential for further improvement. For instance, co-feed CFP of biomass and plastics with ZSM-5 usually produces considerable amounts of lower $C_1$–$C_5$ linear alkanes [12], which are less valuable products than olefins and aromatic hydrocarbons [3,26,27]. Moreover, polyaromatic hydrocarbons, which are generally considered undesirable products due to their low value and high toxicity and mutagenicity [1,13,15,28,29], usually constitute significant fractions of the final aromatic products in co-feed CFP [12]. It is therefore, highly desirable to decrease the yields of alkanes and polyaromatics in co-feed CFP, thus, improving the product distribution toward more valuable monoaromatic hydrocarbons and olefins.

To this end, we proposed gallium (Ga) containing MFI zeolites as the catalysts for co-feed CFP of biomass with plastics. Previous studies have shown that impregnation of conventional aluminosilicate MFI zeolites (i.e., ZSM-5) with Ga (referred as Ga/ZSM-5 hereafter) or incorporation of Ga into the framework of MFI zeolites (e.g., galloaluminosilicate and gallosilicate of ZSM-5 type, referred as Ga–Al–Si and Ga–Si hereafter, respectively) can significantly enhance the conversion of lower alkanes to olefins and aromatic hydrocarbons [26,30–33]. This improvement is mainly because Ga species can significantly improve the dehydrogenation activity of zeolites, and catalyze alkane transformation to olefins and subsequent olefin transformation to aromatics [31–35]. We thus, anticipated that Ga-containing MFI zeolites may be able to enhance petrochemical production in co-feed CFP of biomass and plastics by enhancing alkane transformation to olefins and aromatics.

Furthermore, we hypothesized that Ga-containing zeolites may decrease polyaromatic formation in co-feed CFP of biomass and plastics as compared to conventional ZSM-5 zeolites. Previous studies have indicated that during the preparation of Ga-containing MFI zeolites (e.g., impregnation and calcination), different Ga-oxides (e.g., $Ga_2O_3$ and $GaO^+$) may form and deposit at the pore mouth or in the channels of Ga-containing zeolites [26,30,33,36]. This would decrease the effective pore size of Ga-containing MFI zeolites as compared to that of conventional ZSM-5 zeolites [30,36]; note that the effective pore size of zeolite is conventionally defined as the largest molecule able to pass through the pore [37]. Because polyaromatics generally have a larger molecular size than monoaromatics [29,38], we anticipated that when the pore narrowing of Ga-containing zeolites is properly controlled, Ga-containing zeolites may be able to inhibit the formation of relatively bulkier polyaromatic hydrocarbons (e.g., naphthalenes) while still maintaining the production of valuable monoaromatic hydrocarbons (e.g., benzene, toluene, and *p*-xylene) via shape selective catalysis mechanisms.

To test these hypotheses, we prepared a series of Ga-containing MFI (Ga/ZSM-5, Ga–Al–Si, and Ga–Si) zeolites and tested their catalytic performance in co-feed CFP of pine wood with LDPE. The effects of Ga incorporation on the acidity and structural properties of MFI zeolites were examined using various techniques. CFP of pine wood, LDPE, and their mixtures with conventional ZSM-5 and Ga-containing zeolites were then compared to evaluate the effects of Ga incorporation on the product distribution in co-feed CFP of biomass and plastics.

## 2. Experimental

### 2.1. Materials

Pine wood sawdust was acquired from a furniture factory in Beijing. LDPE powder ($d < 0.105$ mm) was purchased from Li Yang Technology Corporation (Shanghai, China). The conventional ZSM-5 zeolite ($SiO_2/Al_2O_3$ ratio of 25, H type, $d_{50}$ of 2 μm) was shipped from the Catalyst Plant of Nankai University (Tianjin, China). All samples (pine wood, LDPE, and catalysts) were (crushed and) sieved through a 140 mesh (0.105 mm) sieve, and then stored in a desiccator before use. Elemental composition of pine wood and LDPE were analyzed with an elemental analyzer (CE-440, Exeter Analytical, Inc., North Chelmsford, MA) [12].

### 2.2. Catalyst synthesis

The Ga/ZSM-5 zeolites were prepared using incipient wetness method [26,39]. The conventional ZSM-5 was impregnated with an aqueous solution of $Ga(NO_3)_3$ of appropriate concentrations to yield Ga/ZSM-5 zeolites with the mass fraction ratio of $Ga_2O_3$–ZSM-5 of 2, 5, and 8 wt.%. During the impregnation, the solution was stirred at room temperature for 2 h, and then kept stirring at 60 °C until water was evaporated. After the impregnation treatment, the zeolites were dried over night at 110 °C, and then calcined at 550 °C for 5 h in air.

The Ga–Al–Si and Ga–Si MFI zeolites were synthesized using the procedure described by Leth et al. [40]. Tetrapropylammonium hydroxide (TPAOH, Aladdin), silica gel ($SiO_2$, Aladdin), $Ga(NO_3)_3$ ($Ga_2O_3$, Aladdin), aluminum isopropoxide ($Al_2O_3$, Aladdin), and deionized water were used as precursor solutions. The starting composition of synthesis gel was $25SiO_2$: $aGa_2O_3$: $bAl_2O_3$: $1Na_2O$: 5TPAOH: $1500H_2O$ (for Ga–Al–Si zeolites: $a+b=1$, $a/b=1$ or 2; for Ga–Si zeolites: $b=0$, $a=0.5$ or 1). The homogeneous gel was transferred into a Teflon-lined stainless-steel autoclave, and then heated at 180 °C under autogenous pressure for 70 h. After the synthesis, the resultant materials were filtered and washed thoroughly with deionized water. The obtained product was dried at 110 °C overnight, and then calcined at 550 °C for 5 h to remove the organic template. Finally, the synthesized zeolites were converted to H-form catalysts by ion exchange with $NH_4NO_3$ solution (1.0 M) for three times, followed by filtration, drying at 110 °C overnight, and calcination under air at 550 °C for 5 h.

### 2.3. Catalyst characterizations

X-ray diffraction patterns of the zeolites were recorded using a Bruker D8 Advanced powder X-RAY diffractometer using CuKα radiation at 40 kV and 40 mA. The chemical composition of synthesized zeolites were determined by X-ray fluorescence (XRF) using a spectrometer (XRF-1800, Shimadzu Co., Japan). The textural properties of the zeolites were characterized by $N_2$ adsorption at −196 °C on a Quantachrome Autosorb-iQ$^2$ instrument. The zeolites were outgassed at 300 °C under vacuum before $N_2$ adsorption. Micropore volume was calculated using the *t*-plot method on the adsorption branch.

Pyridine FT-IR analyses were performed using a Nicolet 5700 spectrometer. The zeolites were pressed into self-supporting wafers (10 mg, 13 mm diameter). The zeolite wafers were then activated in situ in an IR cell at 400 °C under vacuum for 2 h. Thereafter, the temperature of IR cell was decreased to 100 °C and the background spectra of the zeolites were recorded. Pyridine was adsorbed on the sample for 10 min, followed by desorption at 200 °C. The concentrations of Brönsted and Lewis acid sites were then calculated on the basis of the intensity of the 1540 $cm^{-1}$ (Brönsted) and 1450 $cm^{-1}$ (Lewis) bands.

**Table 1**
Characterizations of the ZSM-5 and Ga-containing MFI zeolites.

| Catalyst | $Ga_2O_3$[a] (%) | $SiO_2/Ga_2O_3$[a] | $SiO_2/Al_2O_3$[a] | $SiO_2/(Al_2O_3+Ga_2O_3)$ | $S_{BET}$[b] ($m^2/g$) | $V_{micro}$[c] ($cm^3/g$) | $A_{Brönsted}$[d] (μmol/g) | $A_{Lewis}$[d] (μmol/g) |
|---|---|---|---|---|---|---|---|---|
| ZSM-5 | – | – | 25.5 | 25.5 | 403.3 | 0.161 | 420.3 | 134.0 |
| 5Ga/ZSM-5 | 4.37 | 63.73 | 24.5 | 17.7 | 372.6 | 0.138 | 251.9 | 114.2 |
| Ga–Al–Si1 | 4.67 | 61.1 | 40.3 | 24.3 | 330.5 | 0.124 | 157.4 | 126.9 |
| Ga–Al–Si2 | 6.08 | 47.1 | 73.5 | 28.7 | 336.3 | 0.119 | 141.8 | 101.1 |
| Ga–Si1 | 8.58 | 33.2 | – | 33.2 | 355.6 | 0.132 | 132.4 | 118.8 |
| Ga–Si2 | 6.13 | 47.7 | – | 47.7 | 388.3 | 0.149 | 141.1 | 54.5 |

[a] By XRF analysis.
[b] From $N_2$ adsorption measurements (BET method).
[c] From $N_2$ adsorption measurements (*t*-plot).
[d] Measured by IR spectrum of adsorbed pyridine.

Temperature-programed reduction of $H_2$ ($H_2$-TPR) was conducted with the Micromeritics Autochem 2920 instrument. About 0.1 g of the zeolite was pretreated at 550 °C for 1 h in He stream. After cooling the zeolite to 100 °C in He stream, the reduction was performed in a mixture of 10% $H_2$/Ar flowing at a heating rate of 15 °C/min up to 1000 °C. Hydrogen consumed during TPR run was detected by a thermal conductivity detector (TCD).

### 2.4. Catalytic fast pyrolysis

CFP tests were conducted with a semi-batch microreactor (Pyroprobe 5200, CDS Analytical, Inc.) using a protocol described elsewhere [12,41]. To prepare the samples for CFP tests, zeolite catalysts were thoroughly mixed with a particular reactant (pine wood, LDPE, and their co-feed mixture (mass ratio of 2)) in a catalyst-to-reactant ratio of 15. It is noted that due to the small reactor and sample size used in CDS pyroprobe pyrolysis, high catalyst-to-reactant ratios (e.g., 10–20) are required to ensure that biomass- and plastic-derived volatile intermediates can be further effectively converted within the catalyst matrix to final products before the volatile intermediates evolve out of the pyroprobe reactor (see Supplementary data for more discussion on catalyst-to-reactant ratios) [15,42,43]. Approximately 4 mg of the mixtures were placed into the pyroprobe. The samples were then rapidly heated to 550 °C at a heating rate of 20 °C/ms, and held for 60 s under high-purity helium flux during fast pyrolysis. The volatiles emitted via this fast heating were carried by helium through a heated transporting tube (300 °C) to a gas chromatograph (Agilent 7890A) that was equipped with a mass spectrometer (5975C MSD), a flame ionization detector (FID), and a thermal conductivity detector (TCD). The condensable pyrolysis products were separated with an HP-Innowax column (30 m × 0.25 mm i.d. × 0.25 μm film thickness, Agilent Technologies, Inc.). The non-condensable gases were separated with a fused silica capillary column (HP-Plot/Q, 30 m × 0.32 mm i.d. × 20 μm film thickness, Agilent Technologies, Inc.). For tentative identification of pyrolysis products, all mass spectra were compared to the NIST mass spectrum library. The yields of hydrocarbons (alkanes, olefins, and aromatics) and carbon oxides (CO and $CO_2$) were quantified with FID and TCD, respectively. Triplicate CFP tests were performed for the condensable and non-condensable product analyses, respectively. The carbon contents in the spent catalysts were measured in triplicate using the elemental analyzer to determine the solid (char/coke) yield in CFP tests. All yields are reported in terms of carbon yield (moles of carbon atoms in the products relative to those in the reactants, Eq. (1)). Aromatic and xylene selectivity are calculated according to Eqs. (2) and (3), respectively.

$$\text{Carbon yield} = \frac{\text{Moles of carbon in a product}}{\text{Moles of carbon in reactant}} \times 100\% \quad (1)$$

$$\text{Aromatic selectivity} = \frac{\text{Moles of carbon in an aromatic product}}{\text{Moles of carbon in all aromatic products}} \times 100\% \quad (2)$$

$$\text{Xylene selectivity} = \frac{\text{Moles of a xylene isomer}}{\text{Moles of all xylene isomer}} \times 100\% \quad (3)$$

## 3. Results and discussion

### 3.1. Catalyst characterizations

Preliminary tests showed that Ga/ZSM-5 impregnated with different amounts of Ga (2–8 wt.%) yielded similar product distributions in co-feed CFP of biomass (cellulose) and LDPE mixtures (see Figs. S1 and S2 in Supplementary data (SD)). In contrast, the amount of Ga incorporated into the framework of Ga–Al–Si and Ga–Si MFI zeolites had a significant influence on the product distribution in the co-feed CFP. Therefore, ZSM-5 impregnated with 5 wt.% (5Ga/ZSM-5), as well as Ga–Al–Si and Ga–Si zeolites with different Ga contents were selected for further characterizations and CFP evaluations.

The bulk Ga content (as $Ga_2O_3$) of the Ga-containing zeolites were measured with XRF techniques and are reported in Table 1. Previous studies have indicated that due to the large size of hydrated $Ga^{3+}$ cations, Ga is unlikely to enter the pores or framework positions of ZSM-5 during impregnation or ion-exchange [26,33]. Therefore, Ga/ZSM-5 zeolites prepared with incipient wetness method contain mainly non-framework $Ga_2O_3$ dispersed on the external surface of zeolites [26,33]. In contrast, Ga–Al–Si and Ga–Si zeolites contains both framework and non-framework Ga species because some framework Ga would undergo degalliation to form non-framework Ga-oxides (e.g., $Ga_2O_3$ and $GaO^+$) in the channels and on the external surface of the zeolites during the zeolite calcination and conversion to H-form zeolites [30,33,36]. As a result, the bulk Ga contents reported in Table 1 included both framework and non-framework Ga species.

The existing forms of non-framework Ga-oxides were examined with $H_2$-TPR analyses. As shown in Fig. 1, the conventional ZSM-5 exhibited no hydrogen reduction peak in the $H_2$-TPR profiles. In contrast, significant hydrogen reduction peaks were observed for the Ga-containing zeolites. These peaks are attributed to hydrogen consumption for the reduction of non-framework Ga species since the framework $Ga^{3+}$ species (as the case of other framework metals) cannot be reduced at the tested temperature range [27,33,44,45]. The two major $H_2$ consumption peaks at ~600 °C and ~900–950 °C can be mainly attributed to the reduction of non-framework $Ga_2O_3$ to $Ga_2O$ and $GaO^+$ to $Ga^+$, respectively [45,46]. The $H_2$-TPR profile of 5Ga/ZSM-5 exhibited the highest $Ga_2O_3$ peak and the lowest $GaO^+$ peak among the Ga-containing ZSM-5 zeolites,

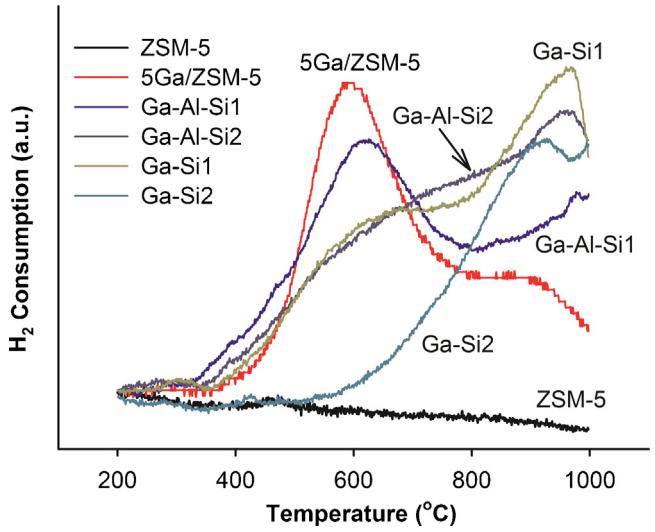


**Fig. 1.** $H_2$-TPR profiles for the ZSM-5 and Ga-containing MFI zeolites.

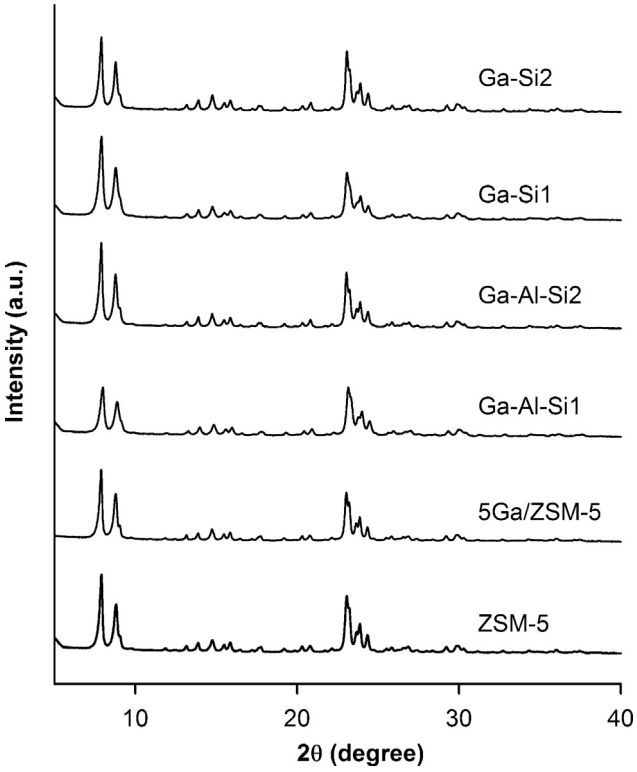


**Fig. 2.** XRD patterns of the ZSM-5 and Ga-containing MFI zeolites.

consistent with the previous finding that Ga/ZSM-5 zeolites contain predominantly $Ga_2O_3$ [26,33]. For Ga–Al–Si1, which had the lowest Ga content (4.67 wt.%) among the hydrothermally synthesized Ga-containing zeolites, the first peak is more pronounced than the second one, indicating that its non-framework Ga is mainly present as well-dispersed $Ga_2O_3$. In comparison, the second peak becomes more pronounced for the other three hydrothermally synthesized Ga-containing zeolites. This result agrees well with the previous finding that degalliation of Ga–Al–Si and Ga–Si zeolites results in a mixture of Ga-oxides (e.g., $Ga_2O_3$ and $GaO^+$), and $GaO^+$ ions are favored at high Ga loading [26,33]. It is noted that no evident peak for the reduction of well-dispersed $Ga_2O_3$ (~600 °C) was observed for Ga–Si2. This is probably because the degalliation of Ga–Si2 is not very significant due to its high $SiO_2/Ga_2O_3$ ratio [26,30].

All Ga-containing zeolites had essentially the same XRD patterns as the conventional ZSM-5 zeolite, exhibiting the characteristic peaks of MFI type zeolite at the ~8° and 23° (Fig. 2). This result indicates that the framework of the Ga-containing zeolites are the same as that of ZSM-5. Additionally, no peaks of bulk Ga-oxides are observed in the XRD profiles of Ga-containing zeolites, indicating that non-framework Ga-oxides were well dispersed on the channel walls or external surfaces of zeolites [28,45,47].

$N_2$-adsorption/desorption results show that Ga-containing zeolites had a smaller BET surface area and micropore volume than the conventional ZSM-5 (Table 1). This result is consistent with the previous observations that Ga incorporation will decrease the surface area and pore volume of zeolites [26,33,39,47]. For Ga/ZSM-5, this decrease can be mainly attributed to the partial blockage of zeolite pore mouths by extracrystalline $Ga_2O_3$ (since Ga cannot enter the channel of ZSM-5 during impregnation) [26,39,46,48]. In comparison, the decrease in surface area and pore volume of Ga–Al–Si and Ga–Si zeolites is mainly due to the occupation of a part of channel space by the non-framework Ga-oxide species formed during degalliation [26,33,36]. For Ga–Si2, its pore volume and surface area were just slightly smaller than those of ZSM-5, agreeing with the result of $H_2$-TPR analyses that insignificant amounts of non-framework $Ga_2O_3$ oxides were created from the degalliation of Ga–Si2.

Acidity analyses by pyridine adsorption show that the density of Brönsted acid sites decreased considerably for the Ga-containing zeolites, especially for the Ga–Al–Si and Ga–Si zeolites (Table 1). This decrease can be partly attributed to the replacement of some Brönsted acid sites by Ga [47,48]. In addition, previous studies have indicated that Brönsted acid sites are mainly associated with framework Al and Ga (i.e., bridged silanol groups (Si–OH–Al) and gallium species (Si–OH–Ga)), and the Si–OH–Ga sites are more covalent than Si–OH–Al sites [26,33]. Therefore, Ga–Al–Si and especially Ga–Si zeolites usually have much lower Brönsted acidity than conventional ZSM-5 zeolites [30,33,49]. Compared with the Brönsted acidity, the Lewis acidity decreased less significantly for the Ga-containing zeolites (this is with the exception of Ga–Si2 see Table 1). Previous work has indicated that Lewis acid sites of zeolites are mainly associated with non-framework Al and Ga species [26,33], and for Ga–Al–Si and Ga–Si zeolites, their Lewis acid sites are correlated to the amounts of non-framework $Ga_2O_3$ generated during zeolite calcination [30,33,45]. This explains why Ga–Si2 had a much weaker Lewis acidity (54.5 μmol/g) than the other Ga–Al–Si and Ga–Si zeolites (101.1–126.9 μmol/g), since it had the lowest non-framework $Ga_2O_3$ among the Ga–Al–Si and Ga–Si MFI zeolites (as manifested from the $H_2$-–TPR profiles in Fig. 1).

The characterization results reported herein are generally in line with the previous finding that Ga modification can considerably change the pore structure and acidity of zeolites, and the route for preparing Ga-containing zeolites (impregnation with Ga or incorporation of Ga into the zeolite framework) has a significant influence on the forms and locations of Ga species on the zeolites [26,33,36,47–49]. This, in turn, significantly influenced the product distribution in CFP of pine wood, LDPE, and their mixtures, which are discussed below.

### 3.2. *CFP of pine wood and LDPE with ZSM-5 and Ga-containing zeolites*

Co-feed CFP of pine wood and LDPE mixtures (mass ratio 2:1) with ZSM-5 and Ga-containing zeolites produced similar final major products, which can generally be classified into five groups: aromatic hydrocarbons (monoaromatics and polyaromatics), $C_2$–$C_5$ olefins, $C_1$–$C_5$ alkanes, carbon oxides (CO and $CO_2$), and solid residue (char and coke) (see Table 2). Note that due to the

**Table 2**
Detailed product yields in co-feed CFP of pine wood and LDPE mixture (mass ratio of 2) with the ZSM-5 and Ga-containing MFI zeolites.

| Carbon yield (C%) | ZSM-5 | 5Ga/ZSM-5 | Ga–Al–Si1 | Ga–Al–Si2 | Ga–Si1 | Ga–Si2 |
|---|---|---|---|---|---|---|
| Aromatic hydrocarbons | | | | | | |
| Benzene | 3.53 ± 0.04 | 4.41 ± 0.38 | 5.13 ± 0.05 | 4.96 ± 0.29 | 3.95 ± 0.33 | 2.03 ± 0.15 |
| Toluene | 9.21 ± 0.04 | 11.3 ± 0.77 | 12.6 ± 0.16 | 12.9 ± 0.42 | 11.1 ± 1.12 | 7.13 ± 0.41 |
| Ethylbenzene | 0.59 ± 0.00 | 0.67 ± 0.03 | 0.82 ± 0.00 | 0.83 ± 0.04 | 1.15 ± 0.13 | 1.06 ± 0.06 |
| *p*-Xylene | 2.43 ± 0.00 | 3.64 ± 0.21 | 5.41 ± 0.01 | 6.63 ± 0.15 | 7.73 ± 0.82 | 3.27 ± 0.20 |
| *m*-Xylene | 4.42 ± 0.04 | 4.59 ± 0.38 | 2.15 ± 0.05 | 0.52 ± 0.03 | 1.32 ± 0.15 | 4.11 ± 0.23 |
| *o*-Xylene | 1.77 ± 0.01 | 1.18 ± 0.11 | 0.57 ± 0.01 | 0.12 ± 0.01 | 0.36 ± 0.04 | 1.57 ± 0.09 |
| 1,2,4-Trimethylbenzene | 0.88 ± 0.00 | 0.28 ± 0.03 | 0.14 ± 0.00 | 0.05 ± 0.00 | 0.18 ± 0.02 | 2.34 ± 0.11 |
| Indane | 0.37 ± 0.00 | 0.28 ± 0.02 | 0.26 ± 0.00 | 0.15 ± 0.01 | 0.32 ± 0.04 | 0.86 ± 0.05 |
| Indene | 0.18 ± 0.00 | 0.27 ± 0.02 | 0.23 ± 0.00 | 0.16 ± 0.02 | 0.24 ± 0.02 | 0.39 ± 0.02 |
| Naphthalene | 1.37 ± 0.03 | 1.25 ± 0.15 | 1.49 ± 0.01 | 1.09 ± 0.06 | 0.86 ± 0.09 | 0.49 ± 0.03 |
| 1-Methylnaphthalene | 0.43 ± 0.01 | 0.14 ± 0.03 | 0.01 ± 0.00 | 0.00 ± 0.00 | 0.01 ± 0.00 | 0.02 ± 0.00 |
| 2-Methylnaphthalene | 1.50 ± 0.02 | 1.06 ± 0.12 | 0.75 ± 0.01 | 0.41 ± 0.01 | 0.54 ± 0.07 | 0.80 ± 0.05 |
| 2,7-Dimethylnaphthalene | 1.55 ± 0.01 | 0.45 ± 0.05 | 0.29 ± 0.01 | 0.14 ± 0.00 | 0.20 ± 0.02 | 0.87 ± 0.03 |
| Olefins | | | | | | |
| Ethylene | 3.09 ± 0.17 | 3.31 ± 0.02 | 3.87 ± 0.09 | 4.26 ± 0.00 | 4.60 ± 0.02 | 5.27 ± 0.06 |
| Propene | 4.02 ± 0.40 | 4.18 ± 0.11 | 4.90 ± 0.17 | 5.60 ± 0.10 | 7.83 ± 0.14 | 11.8 ± 0.32 |
| $C_4$ olefins | 5.28 ± 0.48 | 2.94 ± 0.02 | 4.34 ± 0.20 | 4.73 ± 0.03 | 5.84 ± 0.24 | 9.41 ± 0.26 |
| $C_5$ olefins | 1.80 ± 0.24 | 1.43 ± 0.01 | 1.48 ± 0.10 | 1.64 ± 0.00 | 2.37 ± 0.14 | 4.19 ± 0.03 |
| Alkanes | | | | | | |
| Methane | 0.65 ± 0.02 | 0.72 ± 0.00 | 1.36 ± 0.00 | 1.22 ± 0.04 | 0.91 ± 0.01 | 0.69 ± 0.01 |
| Ethane | 0.58 ± 0.05 | 0.39 ± 0.00 | 0.56 ± 0.00 | 0.53 ± 0.03 | 0.30 ± 0.01 | 0.28 ± 0.01 |
| Propane | 8.30 ± 0.65 | 5.10 ± 0.09 | 5.72 ± 0.13 | 5.29 ± 0.04 | 2.36 ± 0.03 | 2.44 ± 0.02 |
| $C_4$ alkanes | 8.12 ± 0.26 | 6.33 ± 0.03 | 3.73 ± 0.18 | 3.16 ± 0.14 | 2.43 ± 0.12 | 2.26 ± 0.04 |
| $C_5$ alkanes | 3.04 ± 0.20 | 2.12 ± 0.04 | 1.41 ± 0.08 | 1.12 ± 0.06 | 1.14 ± 0.07 | 1.04 ± 0.00 |
| CO and $CO_2$ | 10.9 ± 0.96 | 10.0 ± 0.24 | 8.91 ± 0.18 | 11.4 ± 1.18 | 8.65 ± 0.32 | 7.93 ± 0.17 |
| Char/coke | 26.2 ± 0.36 | 25.0 ± 0.30 | 24.9 ± 2.33 | 24.1 ± 2.93 | 26.8 ± 0.53 | 23.5 ± 0.18 |

high catalyst-to-reactant ratio (15) used in the CFP tests, biomass-derived oxygenates (e.g., aldehydes, acids, and phenols) were only intermittently detected at negligible amounts in the final product streams, indicating that they are almost completely converted to the five groups of final products listed in Table 2 [12,15,42,43].

As shown in Fig. 3, the product distributions were considerably affected by the catalysts used in the co-feed CFP process. Compared with the conventional ZSM-5 zeolite, all Ga-containing zeolites (Ga/ZSM-5, Ga–Al–Si, and Ga–Si) considerably decreased the yield of alkanes and polyaromatics (Fig. 3). These decreases are mainly balanced by the increases in olefins and/or monoaromatic hydrocarbons. Consequently, the overall yield of desirable petrochemicals (monoaromatics plus olefins) increased remarkably from 37.6 C% for ZSM-5 to 38.8 C% for 5Ga/ZSM-5 and 41.9–53.4 C% for the Ga–Al–Si and Ga–Si MFI zeolites in the co-feed CFP. In addition, it is noticed that the yield of char/char was generally comparable for all catalysts tested in this study, suggesting that Ga incorporation does not considerably influence char/coke formation in co-feed CFP (see SD for more discussion).

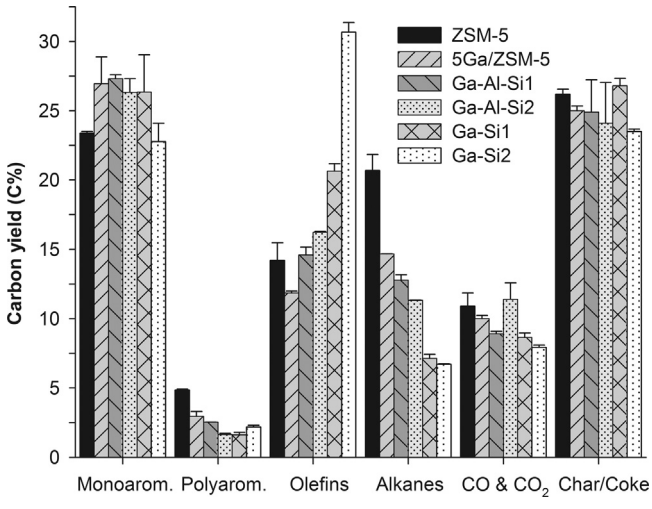


**Fig. 3.** Carbon yields of major products from catalytic fast pyrolysis of pine wood and LDPE mixture (mass ratio of 2) with the ZSM-5 and Ga-containing MFI zeolites.

The result confirms that Ga modification, especially incorporation of Ga into the framework of MFI zeolites, can greatly enhance the conversion of less valuable lower alkanes to more valuable petrochemicals (monoaromatics and olefins). Compared with the conventional ZSM-5, Ga-containing zeolites also considerably decreased the yield of undesired polyaromatics in the co-feed CFP. As a result, the Ga-containing zeolites greatly improved the bulk product distribution toward more valuable products in co-feed CFP.

To get more insight into this improvement, CFP of pine wood and LDPE individually with ZSM-5 or Ga-containing zeolites were also investigated. Fig. 4(a) shows that CFP of LDPE alone with ZSM-5 produced a much higher alkane yield (45.2 C%) than monoaromatic hydrocarbons (19.0 C%) and olefins (24.7 C%) (see SD for detailed product lists). However, when Ga-containing zeolites were used as the catalysts, the yields of alkanes were significantly decreased, while the yields of monoaromatic hydrocarbons and/or olefins were considerably improved (Fig. 4(a)). These trends are the same as those observed in co-feed CFP of pine wood and LDPE (Fig. 3).

On the other hand, Ga-modification had less pronounced effects on the product distribution from CFP of pine wood alone. As shown in Fig. 4(b), the Ga-containing zeolites decreased the yields of polyaromatics and alkanes in CFP of pine wood alone, similar to what has been observed in co-feed CFP of pine wood with LDPE (Fig. 3). However, the yields of of monoaromatic hydrocarbons, olefins, and char/coke are not significantly different for the conventional ZSM-5 and Ga-containing zeolites.

Based on the above comparisons, it can be discerned that Ga-containing zeolites improve petrochemical production in co-feed CFP of pine wood and LDPE mixture mainly by enhancing the conversion of LDPE-derived alkanes to olefins and/or monoaromatic hydrocarbons. Indeed, previous studies have shown that during catalytic cracking of LDPE over zeolites, significant amounts of alkanes can be formed from the thermal and catalytic cracking of LDPE, as well as subsequent acid-catalyzed

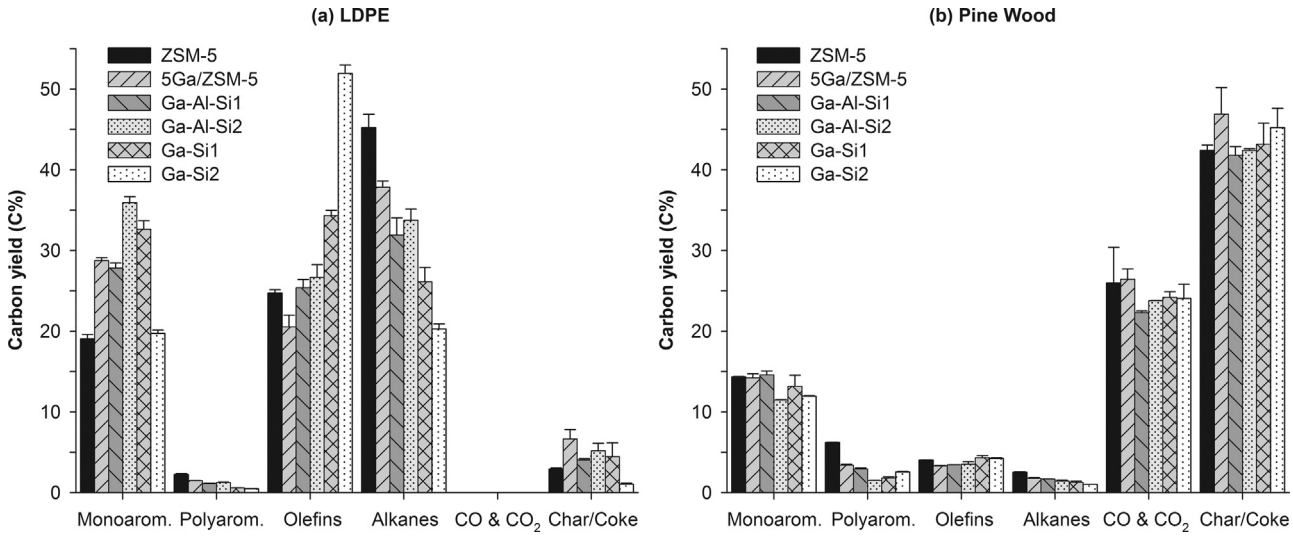


**Fig. 4.** Carbon yields of major products from catalytic fast pyrolysis of (a) LDPE alone, and (b) pine wood alone with the ZSM-5 and Ga-containing MFI zeolites.

hydride transfer reactions through which LDPE-derived olefins are transformed to aromatic hydrocarbons [21,23,31,32,35]. However, ZSM-5 is not effective at converting alkanes to olefins, which is the first and limiting step of alkane aromatization [32]. Consequently, alkanes constituted a significant fraction of the final products from CFP of LDPE and co-feed CFP of pine wood and LDPE mixtures with ZSM-5 (see Fig. 3 and Fig. 4(a)). In comparison, Ga-containing zeolites, especially Ga–Al–Si and Ga–Si zeolites, significantly decreased alkane yields and increased olefin and/or monoaromatic hydrocarbon yields in CFP. This change can be attributed to the fact that non-framework Ga-oxides (e.g., $Ga_2O_3$ and $GaO^+$) in Ga-containing zeolites (in cooperation with Brönsted acid sites) can catalyze the dehydrogenation of alkanes to olefins by providing new dehydrogenation routes (see SD Fig. S3) [32,35]. In addition, non-framework Ga species can also catalyze subsequent dehydrogenation reaction steps that lead to the conversion of olefins to aromatic hydrocarbons (e.g., olefins to dienes and cyclic diolefins to aromatics) [31,32,34]. Therefore, Ga-containing zeolites (Ga/ZSM-5, Ga–Al–Si, and Ga–Si zeolites) significantly increase the yields of olefins and/or monoaromatic hydrocarbons at the expense of alkanes in co-feed CFP of pine wood with LDPE (Fig. 3). In addition, similar to what has been observed in alkane aromatization processes [26,33,36], Ga–Al–Si and Ga–Si zeolites prepared with hydrothermal synthesis exhibited higher catalytic activity for converting alkanes to petrochemicals (monoaromatics and olefins) than Ga/ZSM-5 zeolites prepared with incipient wetness method (Fig. 3).

It is noticed that Ga–Si2 zeolite produced the highest yield of olefins, but the lowest yields of aromatics and alkanes among Ga-containing zeolites tested in co-feed CFP of pine wood with LDPE (Fig. 4). This result suggests that Ga–Si2 can effectively convert LDPE-derived alkanes to olefins, but is ineffective at their subsequent aromatization. In contrast, an opposite trend was observed for 5Ga/ZSM-5, which produced the highest monoaromatic and alkane yields but the lowest olefin yield among Ga-containing zeolites. This result implies that 5Ga/ZSM-5 is not very effective at converting alkanes to olefins, but can effectively convert olefins to aromatics. Considering that the non-framework Ga-oxides were composed mainly of $GaO^+$ and insignificant amounts of $Ga_2O_3$ for

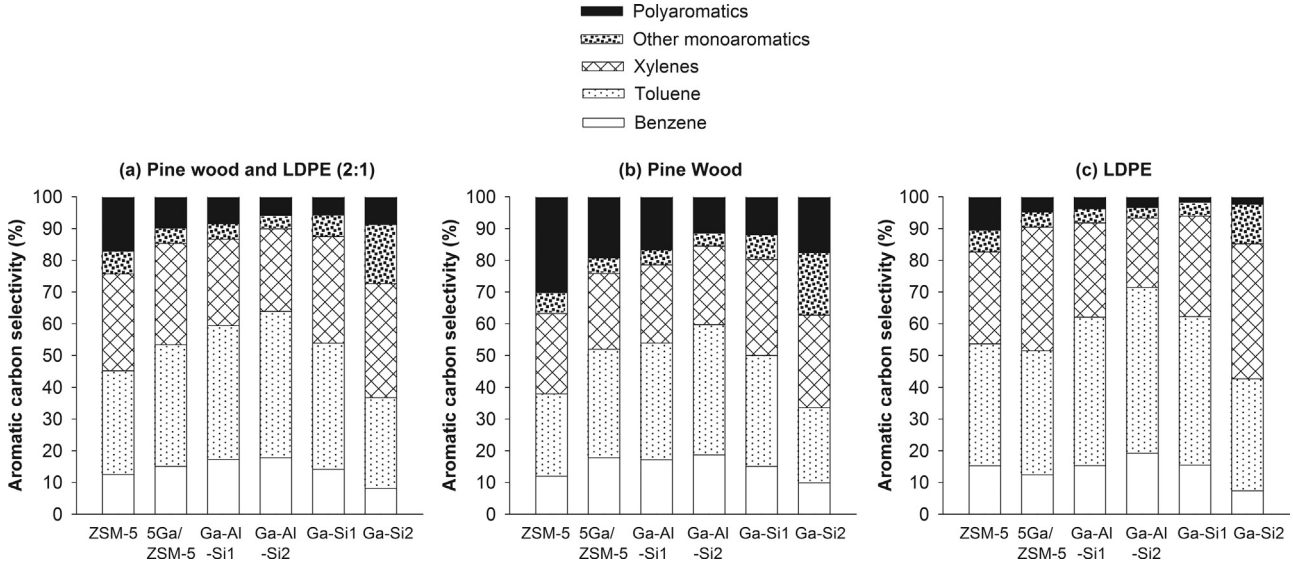


**Fig. 5.** Aromatic selectivity in catalytic fast pyrolysis of (a) pine wood and LDPE mixture (mass ratio of 2), (b) pine wood, and (c) LDPE with the ZSM-5 and Ga-containing MFI zeolites.

Ga–Si2, whereas, they consisted of predominant $Ga_2O_3$ and minor $GaO^+$ for 5Ga/ZSM-5 (see $H_2$-TPR in Fig. 1), the result suggests that $GaO^+$ may play an important role in activation of alkanes to olefins, but not in olefin aromatization; in contrast, $Ga_2O_3$ may be the main active Ga species for catalyzing olefin aromatization.

Similar in co-feed CFP (Fig. 3), Ga-containing zeolites considerably decreased the yield of undesired polyaromatic hydrocarbons in CFP of pine wood alone and LDPE alone as compared to ZSM-5 (Fig. 4(a) and (b)). As a result, the aromatic product distribution was improved towards more valuable monoaromatic hydrocarbons (e.g., benzene, toluene, and xylenes) in CFP of biomass, plastics, and their mixtures with Ga-containing zeolites (see Fig. 5). This improvement can be probably attributed to the fact that Ga-containing zeolites usually have a smaller effective pore size than conventional ZSM-5 zeolites. Specifically, Ga/ZSM-5 zeolites may have a smaller effective pore size than ZSM-5 because the pore mouths of Ga/ZSM-5 may be partially blocked by extracrystalline $Ga_2O_3$ oxides [2]. On the other hand, Ga–Al–Si and Ga–Si MFI zeolites may have a narrowed channel due to the deposition of non-framework Ga oxides in their channels [36]. Compared with conventional ZSM-5, Ga-containing zeolites may thus, be able to decrease the yields of bulky polyaromatics by inhibiting their formation in the narrowed zeolite pores (for Ga–Al–Si and Ga–Si), or preventing them from diffusing out of the partially blocked pores to constitute the final products (for Ga/ZSM-5).

To further evaluate this inference, we compared the yields in co-feed CFP with Ga-containing zeolite to that with ZSM-5 zeolite for each aromatic product. The ratio reflects whether the production of a given aromatic product is enhanced (if the ratio is >1) or inhibited (if the ratio is <1) when the Ga-containing MFI zeolites were used to replace ZSM-5 as the catalyst in CFP. The ratio for each aromatic product was then plotted against its critical diameter ($d_c$) (see Fig. 6), which is conventionally defined as the diameter of the smallest cylinder that can circumscribe the molecule in its most favorable equilibrium conformation [50] and was calculated using quantum chemical computations (see Table S3 in SD) [38].

As shown in Fig. 6, the ratios are generally >1 for aromatic products with $d_c$ = ~6.7 Å (i.e., benzene, toluene, and *p*-xylene), indicating that their production was enhanced when Ga-containing zeolites were used as the catalyst in CFP (with the exception of Ga–Si2, see discussion below). In contrast, the ratios are generally <1 for aromatic hydrocarbons with $d_c$ > 7.3 Å, indicating that their yields were decreased when Ga-containing zeolites were used. Actually, a general trend can be discerned in the figures that the ratio between the yields in co-feed CFP with Ga-containing zeolites and ZSM-5 zeolite decreases with the increase of the product critical diameter (this is with the exception of Ga–Si2, which will be discussed below). Similar trends are also observed for CFP of pine wood alone and LDPE alone (see Figs. S4 and S5 in SD). This result indicates that the formation of larger aromatic hydrocarbons is increasingly inhibited when Ga-containing zeolites are used as the catalyst in CFP.

For Ga–Si2, Fig. 6(e) shows that while it inhibited the formation of bulky polyaromatic hydrocarbons in CFP, it enhanced mainly the production of some relatively larger monoaromatic hydrocarbons (i.e., indane, indene, and 1,2,4-trimethylbenzene). This is probably because the degalliation of Ga–Si2 was not significant and produced

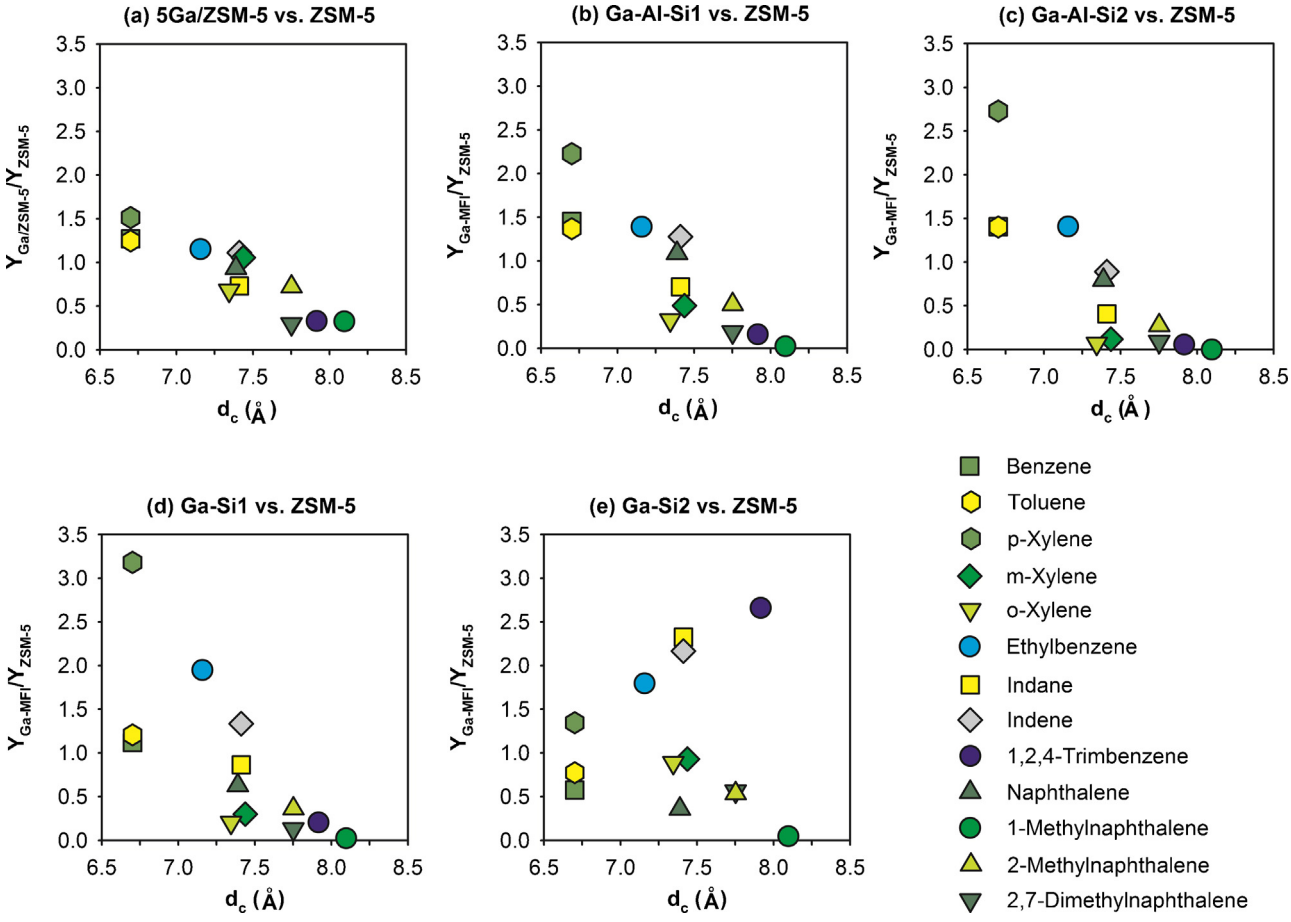


**Fig. 6.** The ratio between the yield of aromatic hydrocarbon products in CFP of pine wood and LDPE mixture (mass ratio 2) with Ga-containing MFI and ZSM-5 zeolites as a function of the molecular size of the aromatics.

only insignificant amounts of non-framework $Ga_2O_3$ in its channels (see $H_2$-TPR profile in Fig. 1). As a result, the effective pore size of Ga–Si2 is only slightly smaller than that of ZSM-5, thus, favoring the formation of relatively larger monoaromatic hydrocarbons.

Notably, the ratios between *p*-xylene ($d_c$ = 6.701 Å) in co-feed CFP with Ga-containing and ZSM-5 zeolites are significantly higher than 1, whereas, the ratios are considerably lower than 1 for *m*-xylene ($d_c$ = 7.437 Å) and *o*-xylene ($d_c$ = 7.345 Å) (with the exception of Ga–Si2, which is discussed below) (see Fig. 6). Similar results are also observed for CFP of pine wood alone and LDPE alone (see Figs. S4 and S5 in SD). This result indicates that Ga-containing zeolites can significantly enhance the production of *p*-xylene over its meta and ortho isomers in CFP as compared to ZSM-5. As a result, both the yield and selectivity for *p*-xylene were significantly improved when CFP was conducted with Ga-containing zeolites (Fig. 7). For Ga–Si2, whose effective pore size is only slightly smaller than ZSM-5, it therefore, just marginally improved the yield and selectivity for *p*-xylene as compared to ZSM-5 (see Fig. 7).

The result shown in Fig. 7 is very promising because *p*-xylene is a much more desirable product than *m*- and *o*-xylenes. Actually, due to its versatile uses and increasing market demands, there is a growing interest in producing *p*-xylene from CFP of biomass [1,2]. However, CFP of biomass with ZSM-5, the most commonly used catalyst in CFP, usually produces only small amounts of *p*-xylene (carbon yield usually <2 C% [2]), similar to what was obtained from CFP of pine wood with ZSM-5 in this study (see Fig. 7(a)). The low yields of *p*-xylene in CFP with ZSM-5 can be mainly attributed to the fact that the pore structure of ZSM-5 does not favor the production of *p*-xylene over its meta and ortho isomers, e.g., the para selectivity was less than 30% when pine wood, LDPE, and their mixtures were catalytically pyrolyzed with ZSM-5 (see Fig. 7).

In comparison, the result presented herein indicates that Ga-containing zeolites can significantly improve *p*-xylene production in CFP (Fig. 7). This improvement can be mainly attributed to the decrease in the effective pore size of Ga-containing zeolites due to partial blockage of the pore mouth of Ga/ZSM-5 or the deposition of Ga-oxides inside the channels of Ga–Al–Si and Ga–Si zeolites. As a result of the pore size reduction, the formation and diffusion of bulkier *m*- and *o*-xylenes ($d_c$ = 7.437 Å and 7.345 Å, respectively) in Ga-containing zeolites is more severely inhibited than *p*-xylene ($d_c$ = 6.701 Å). This promotes the isomerization of *m*- and *o*-xylenes to *p*-xylene, which can then diffuse out of the zeolite pores as the final product. Consequently, Ga-containing zeolites (e.g., Ga–Al–Si2 and Ga–Si1) can significantly improve both the yield and selectivity for *p*-xylene in CFP.

### 3.3. *Effects of preparation route of Ga-containing zeolites on co-feed CFP*

The above results show that both impregnation of ZSM-5 zeolite with Ga (Ga/ZSM-5) and incorporation of Ga into the framework of MFI zeolite (e.g., Ga–Al–Si and Ga–Si) can enhance the conversion of low-value alkanes to valuable olefins and/or monoaromatic hydrocarbons, as well as inhibit the formation of undesired polyaromatics in co-feed CFP of biomass and LDPE mixtures. Ga-containing MFI zeolites thus, significantly improve the product distribution toward more valuable products in co-feed CFP as compared to conventional ZSM-5 zeolites.

In addition, it is noticed that Ga–Al–Si and Ga–Si MFI zeolites generally perform better than Ga/ZSM-5 zeolites in co-feed CFP, producing both higher yields and selectivities for valuable petrochemicals (especially *p*-xylene and olefins) than Ga/ZSM-5 (see Table 3). This result suggests that incorporation of Ga into the framework of MFI zeolites is a better choice than post modification of ZSM-5 zeolites with Ga for preparing Ga-containing zeolites used in co-feed CFP of biomass with plastics. This inference is somewhat different from what has been suggested for zeolite modification with Ga in CFP of biomass alone [49]. In fact, previous studies on CFP of biomass employed almost exclusively Ga/ZSM-5 zeolites that were prepared with impregnation or ion exchange method [2,28,39,47–49], and only one study compared CFP of furans with Ga/ZSM-5 and hydrothermally synthesized Ga–Al–Si and Ga–Si zeolites [49]. In this previous study [49], Cheng et al. reported that Ga/ZSM-5 zeolites produced considerably higher aromatic yields than conventional ZSM-5 zeolite in CFP of furan, whereas, Ga–Al–Si and Ga–Si MFI zeolites produced much lower aromatic yields than ZSM-5. They thus, suggested that Ga–Al–Si and Ga–Si MFI zeolites are not suitable catalysts for aromatic production in CFP of biomass because they have lower strong Brönsted acidity than conventional ZSM-5 zeolites [49]. Consistent with this previous inference, the present study shows that Ga–Al–Si and Ga–Si zeolites also decreased overall aromatic yield in CFP of pine wood alone (see Fig. 4(b)). However, Ga–Al–Si and Ga–Si zeolites outperformed the conventional ZSM-5 and Ga/ZSM-5 zeolites in co-feed CFP of biomass and LDPE, producing much higher yields of petrochemicals (monoaromatics plus olefins) than ZSM-5 and 5Ga/ZSM-5 in the co-feed CFP (see Table 3). As described previously, this improvement can be mainly attributed to the higher catalytic activity of Ga–Al–Si and Ga–Si zeolites for converting LDPE-derived alkanes to olefins and/or monoaromatics (see Fig. 3 and Fig. 4(a)).

In addition, the results of Cheng et al. [49] showed that while Ga/ZSM-5 zeolites increased the overall yield of aromatic hydrocarbons in CFP of furan, they increased mainly the yield of undesirable polyaromatics rather than valuable monoaromatics. For example, the aromatic selectivity for polyaromatics (naphthalenes) increased from 10.6% for ZSM-5 to 13.6, 23.5, and 28.1% for the three Ga/ZSM-5 zeolites tested in their study [1]. In contrast, the present study shows that while Ga–Al–Si and GA–Si zeolites increased the yield of monoaromatics in co-feed CFP of pine wood and LDPE mixture, they decreased the yield of polyaromatics by 47.6–66.8% as compared to ZSM-5 (see Fig. 3). The Ga–Al–Si and Ga–Si MFI zeolites thus, improved both the yield and selectivity for valuable monoaromatics in the co-feed CFP.

Regarding *p*-xylene, Cheng et al. reported in another study [2] that ZSM-5 impregnation with Ga (3.8 wt.%) increased *p*-xylene selectivity moderately from 32% for ZSM-5 to 58% for Ga/ZSM-5 in co-feed CFP of 2-methyfuran with propylene and marginally from 53% for ZSM-5 to 58% for Ga/ZSM-5 in CFP of furan alone. Similar improvement was also observed in the present study for CFP of pine wood, LDPE, and their mixture with 5Ga/ZSM-5 (see Table 3). This improvement can be mainly attributed to the partial blockage of pore openings of Ga/ZSM-5 zeolites by Ga-oxides [2]. Cheng et al. further showed that subsequent modification of the Ga/ZSM-5 zeolites with chemical liquid deposition (CLD) of silicon alkoxides increased *p*-xylene selectivity to 96–98% because of more severe blockage of zeolite pore mouth by silicon alkoxides [2]. However, it is noticed that while these Ga-modified zeolites (i.e., Ga/ZSM-5 and Ga/ZSM-5 further modified with silylation) increased *p*-xylene selectivity in CFP of furans, they did not markedly increase *p*-xylene yield compared with conventional ZSM-5 zeolites [2]. In comparison, this present study shows that Ga–Al–Si and Ga–Si MFI zeolites prepared with hydrothermal synthesis method increased significantly both the yield and selectivity for *p*-xylene in CFP of pine wood, LDPE, and their mixtures (see Fig. 7). This result suggests that direct hydrothermal synthesis of Ga–Al–Si and Ga–Si MFI zeolites may provide a more convenient and effective way to improve *p*-xylene production in CFP of biomass, plastics, and their mixtures than post-modification of conventional ZSM-5 with Ga impregnation and CLD silylation.

The above comparisons indicate that Ga–Al–Si and Ga–Si MFI zeolites are more effective catalysts than conventional ZSM-5 and Ga/ZSM-5 zeolites for petrochemical production in co-feed CFP

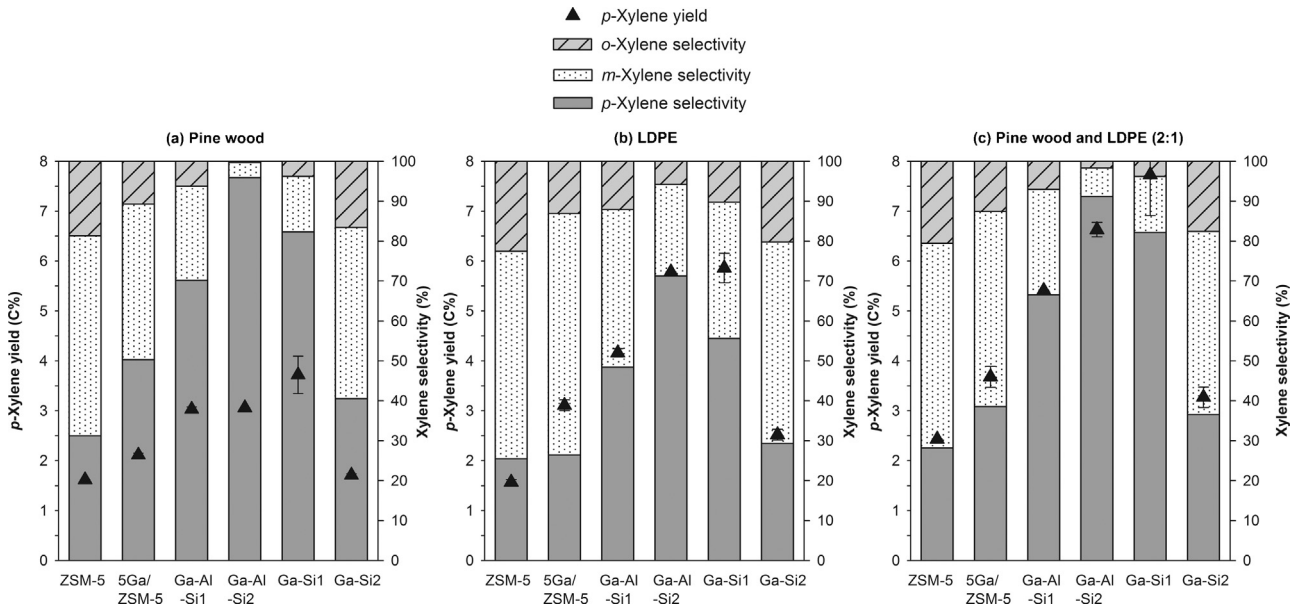


**Fig. 7.** Xylene selectivity and p-xylene yield in CFP of (a) pine wood, (b) LDPE, and (c) their mixture with the ZSM-5 and Ga-containing MFI zeolites.

of biomass with plastics. This can be primarily attributed to the fact that the non-framework Ga species (e.g., $Ga_2O_3$ and $GaO^+$) of Ga–Al–Si and Ga–Si MFI zeolites are mainly distributed uniformly inside the zeolite channels [26,30,33,36]. In contrast, Ga mainly exists as $Ga_2O_3$ particles at the external surface of zeolites or even in a separate phase for Ga/ZSM-5 zeolites [2,33,45]. It is well-known that zeolite catalyzed reactions occur mainly inside the pores of zeolites because the external surface usually accounts for negligible fractions of surface area for zeolite. Consequently, Ga–Al–Si and Ga–Si MFI zeolites can catalyze the conversion of LDPE-derived alkanes to olefins and aromatics much more effectively than Ga/ZSM-5 in the co-feed CFP (see Fig. 3 and Fig. 4(a)), similar to what has been observed in alkane aromatization over Ga-modified zeolites [26,30,33,35,36]. In addition, the deposition of Ga-oxides inside the Ga–Al–Si and Ga–Si MFI channels decreases the effective pore size of the zeolites, and the extent of pore size reduction due to degalliation is generally related to the Si/Ga ratio of Ga–Al–Si and Ga–Si MFI zeolites [30,33,36]. This may provide a simple and viable way to tune the effective pore size of Ga–Al–Si and Ga–Si MFI zeolites, and thus, optimize the product distribution toward more valuable products (e.g., benzene, toluene, and *p*-xylene) via shape selective mechanisms (see Figs. 5 and 7).

### 3.4. Reaction scheme of co-feed CFP of biomass and LDPE with ZSM-5 and Ga-containing MFI zeolites

Many previous studies have indicated that although CFP can rapidly convert biomass into valuable petrochemicals, its carbon efficiency is not very satisfactory when biomass is fed alone in CFP [6,9,12,22]. For example, CFP of pine wood with ZSM-5 produced only 18.4 C% petrochemicals (monoaromatic hydrocarbons plus olefins, Table 3), similar to those reported for woody biomass [5,13,51]. This low carbon efficiency is mainly because natural biomass is deficient in hydrogen and rich in oxygen, it thus,

**Table 3**
Carbon yields of petrochemicals and *p*-xylene and selectivity for monoaromatic hydrocarbon and *p*-xylene in CFP of pine wood, LDPE, and their mixture (2:1) with ZSM-5 and Ga-containing MFI zeolites.

| Feed ratio (wt.%) | | Catalyst | Carbon yield (C%) | | Selectivity (%) | |
|---|---|---|---|---|---|---|
| Pine wood | LDPE | | Petrochemicals[a] | p-Xylene | Monoaromatics[b] | p-Xylene[c] |
| 100 | – | ZSM-5 | 18.4 ± 0.06 | 1.62 ± 0.00 | 69.8 | 31.2 |
| 100 | | 5Ga/ZSM-5 | 17.5 ± 0.55 | 2.11 ± 0.04 | 80.7 | 50.3 |
| 100 | – | Ga–Al–Si1 | 18.0 ± 0.34 | 3.03 ± 0.05 | 83.3 | 70.1 |
| 100 | – | Ga–Al–Si2 | 15.0 ± 0.29 | 3.06 ± 0.00 | 88.6 | 95.9 |
| 100 | – | Ga–Si1 | 17.5 ± 1.16 | 3.72 ± 0.37 | 88.0 | 82.3 |
| 100 | – | Ga–Si2 | 16.2 ± 0.11 | 1.71 ± 0.03 | 82.4 | 40.5 |
| – | 100 | ZSM-5 | 43.7 ± 0.69 | 1.57 ± 0.05 | 89.4 | 25.4 |
| | 100 | 5Ga/ZSM-5 | 49.2 ± 1.07 | 3.11 ± 0.11 | 95.2 | 26.4 |
| – | 100 | Ga–Al–Si1 | 53.2 ± 0.27 | 4.16 ± 0.08 | 96.2 | 48.4 |
| – | 100 | Ga–Al–Si2 | 62.6 ± 0.59 | 5.78 ± 0.00 | 96.7 | 71.3 |
| – | 100 | Ga–Si1 | 66.9 ± 1.21 | 5.86 ± 0.30 | 98.3 | 55.7 |
| – | 100 | Ga–Si2 | 71.7 ± 0.46 | 2.52 ± 0.11 | 97.7 | 29.3 |
| 66.7 | 33.3 | ZSM-5 | 37.6 ± 1.01 | 2.43 ± 0.00 | 82.8 | 28.2 |
| 66.7 | 33.3 | 5Ga/ZSM-5 | 38.8 ± 2.06 | 3.68 ± 0.21 | 90.1 | 38.5 |
| 66.7 | 33.3 | Ga–Al–Si1 | 41.9 ± 0.20 | 5.41 ± 0.01 | 91.5 | 66.5 |
| 66.7 | 33.3 | Ga–Al–Si2 | 42.6 ± 0.74 | 6.63 ± 0.14 | 94.1 | 91.2 |
| 66.7 | 33.3 | Ga–Si1 | 47.0 ± 2.28 | 7.73 ± 0.82 | 94.2 | 82.1 |
| 66.7 | 33.3 | Ga–Si2 | 53.4 ± 1.44 | 3.27 ± 0.20 | 91.3 | 36.5 |

[a] Petrochemicals are the sum of monoaromatics and olefins.
[b] Monoaromatic selectivity is the ratio of monoaromatic yield to overall aromatic yield (monoaromatics and polyaromatics).
[c] *p*-Xylene selectivity is the ratio of *p*-xylene yield to overall xylene yield (*p*-, *m*-, and *o*-xylenes).

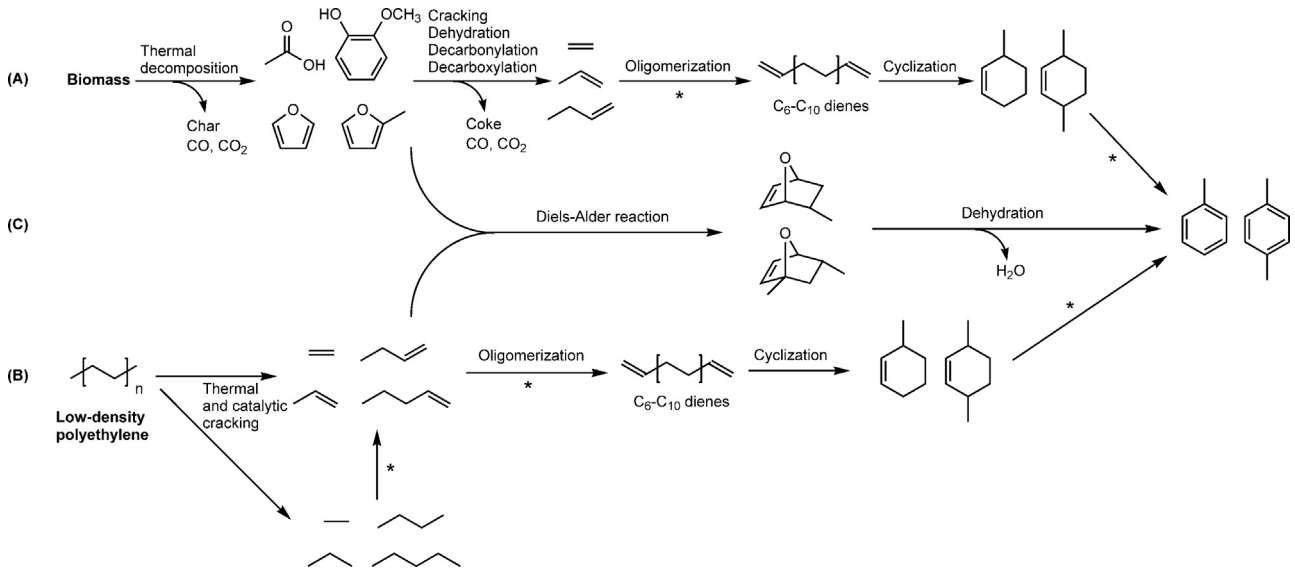


**Fig. 8.** Aromatic formation pathways in co-feed CFP of cellulose and LDPE with Ga-containing MFI zeolites (the reaction steps catalyzed by Ga-oxides are labeled with asterisks (*)).

produces significant amounts of char/coke and carbon oxides during its thermal decomposition and catalytic conversion to olefins and aromatic hydrocarbons (see aromatic formation pathway in CFP of biomass (Route A) in Fig. 8). Consequently, only ~15–35% of the carbon contents of biomass feedstocks can be incorporated into the final aromatic hydrocarbons and olefins in CFP of biomass alone [5,12,14,24,52].

On the other hand, plastics, such as PE and PP are rich in hydrogen and contain no oxygen. They thus, produce insignificant amounts of char/coke and no carbon oxides in CFP, resulting in higher conversion efficiency of their carbon contents into final aromatic and olefin products (Route B in Fig. 8) [12,18,21]. However, CFP of plastics alone usually produces significant amounts of low-value alkanes, which represents a considerable waste of the hydrogen contents of plastics.

To improve petrochemical production in CFP, we have proposed to co-feed hydrogen-deficient biomass with hydrogen-rich plastics in CFP [23]. Various biomass (e.g., cellulose, hemicellulose, and lignin) and plastic (e.g., PE, PP, and PS) mixtures have then been tested in co-feed CFP with ZSM-5 zeolites [9,12,22,23,52,53]. The results indicate that co-feeding of PE (e.g., LDPE and HDPE) with cellulose or natural biomass (e.g., pine wood) that contains considerable cellulose contents can significantly enhance aromatic production in CFP [9,12,22,23,53]. However, this enhancement is not very significant for some other combinations of biomass and plastics (e.g., cellulose/PP and lignin/PE, see SD for more discussion on the selection and mixing ratios of biomass and plastics in co-feed CFP) [9,12,53]. Reaction pathway analyses suggest that the synergy between biomass and plastics for aromatic production is mainly because in the presence of zeolite catalysts, furans (e.g., furan and methylfuran derived from cellulose) can react with linear olefins (e.g., ethylene and propylene derived from PE) via Diels–Alder and dehydration reactions to yield aromatic hydrocarbons (mainly as toluene and xylenes) (see Route C in Fig. 8) [1,54,55]. This route provides a "shortcut" for aromatic formation in co-feed CFP of biomass and plastics [9,12,23]. It can also decrease alkane formation from hydride transfer reactions through which olefins are transformed to aromatic hydrocarbons [23,31,32,35]. Furthermore, Diels–Alder reactions of furans with olefins lead to a change in the deoxygenation pathways of furans from mainly decarbonylation and decarboxylation to dehydration. As a result, more carbon atoms in the furan reactants can be incorporated into the final aromatic products rather than being released as CO and $CO_2$ when biomass is co-fed with plastics in CFP. Consequently, co-feeding of biomass with PE can considerably enhance aromatic production in CFP as compared to CFP of the two feedstocks individually.

Ga-containing MFI zeolites, especially hydrothermally synthesized Ga–Al–Si and Ga–Si MFI zeolites, further improve the production of petrochemicals (olefins and monoaromatic hydrocarbons) in co-feed CFP because non-framework Ga-species formed during degalliation of Ga–Al–Si and Ga–Si MFI zeolites can catalyze the conversion of LDPE-derived alkanes to olefins and subsequent olefins to aromatic hydrocarbons (the reaction steps catalyzed by Ga-oxides are labeled with asterisks in Fig. 8 [31,32]). In addition, because Ga–Al–Si and Ga–Si MFI zeolites had a smaller effective pore size than ZSM-5, they significantly decreased the formation of polyaromatic hydrocarbons in co-feed CFP. The production of more valuable *p*-xylene was also significantly enhanced over its meta and ortho isomers. As a result, the aromatic selectivity was considerably improved toward desirable monoaromatic hydrocarbons (e.g., benzene, toluene, and *p*-xylene) when co-feed CFP was conducted with the Ga–Al–Si and Ga–Si MFI zeolites (see Table 3).

## 4. Conclusions

This study demonstrates that both impregnation of ZSM-5 with Ga (Ga/ZSM-5) and incorporation of Ga into the framework of MFI zeolites (e.g., Ga–Al–Si and Ga–Si MFI) via hydrothermal synthesis can considerably increase the yields of petrochemical products (monoaromatic hydrocarbons and olefins) from co-feed CFP of biomass with LDPE. Further, while Ga-containing zeolites enhanced the production of valuable petrochemicals in the co-feed CFP, they decreased the yields of low-value alkanes and undesired polyaromatic hydrocarbons compared with conventional ZSM-5 zeolites. Ga-containing MFI zeolites can thus, greatly improve the product distribution in co-feed CFP of biomass with plastics.

In addition, the results of this study indicate that the way of preparing Ga-containing zeolites has a significant effect on the catalysts' performance in co-feed CFP of biomass and plastics. Ga–Al–Si and Ga–Si MFI zeolites prepared with hydrothermal synthesis method generally produced both higher yields and selectivities for

valuable petrochemicals (e.g., *p*-xylene and olefins) than Ga/ZSM-5 zeolites prepared with impregnation method. The results indicate that Ga-containing zeolites, especially Ga–Al–Si and Ga–Si MFI zeolites, may be used to increase the carbon efficiency for petrochemical production and improve the product distribution toward more valuable products in co-feed CFP of biomass with LDPE.

## Acknowledgements

This research is supported by the National Key Technology R&D Program (2010BAC66B03) and the special fund of State Key Joint Laboratory of Environment Simulation and Pollution Control (13Y01ESPCT).

## Appendix A. Supplementary data

Supplementary data associated with this article can be found, in the online version, at http://dx.doi.org/10.1016/j.apcatb.2015.02.015.

## References

[1] Y.-T. Cheng, G.W. Huber, Green Chem. 14 (2012) 3114–3125.
[2] Y.T. Cheng, Z.P. Wang, C.J. Gilbert, W. Fan, G.W. Huber, Angew. Chem. Int. Ed. 51 (2012) 11097–11100.
[3] N. Rahimi, R. Karimzadeh, Catal. A: Gen. 398 (2011) 1–17.
[4] A.K. Panda, R.K. Singh, D.K. Mishra, Renew. Sustain. Energy Rev. 14 (2010) 233–248.
[5] P.S. Rezaei, H. Shafaghat, W.M.A.W. Daud, Appl. Catal. A: Gen. 469 (2014) 490–511.
[6] C. Liu, H. Wang, A.M. Karim, J. Sun, Y. Wang, Chem. Soc. Rev. 43 (2014) 7594–7623.
[7] D.P. Serrano, J. Aguado, J.M. Escola, E. Garagorri, J. Anal. Appl. Pyrolysis 58 (2001) 789–801.
[8] G.W. Huber, S. Iborra, A. Corma, Chem. Rev. 106 (2006) 4044–4098.
[9] C. Dorado, C.A. Mullen, A.A. Boateng, ACS Sustain. Chem. Eng. 2 (2014) 301–311.
[10] J.A. Botas, D.P. Serrano, A. García, R. Ramos, Appl. Catal. B: Environ. 145 (2014) 205–215.
[11] T.R. Carlson, T.R. Vispute, G.W. Huber, ChemSusChem 1 (2008) 397–400.
[12] X. Li, J. Li, G. Zhou, Y. Feng, Y. Wang, G. Yu, S. Deng, J. Huang, B. Wang, Appl. Catal. A: Gen. 481 (2014) 173–182.
[13] T.R. Carlson, Y.-T. Cheng, J. Jae, G.W. Huber, Energy Environ. Sci. 4 (2011) 145–161.
[14] D.A. Ruddy, J.A. Schaidle, J.R. Ferrell Iii, J. Wang, L. Moens, J.E. Hensley, Green Chem. 16 (2014) 454–490.
[15] T.R. Carlson, J. Jae, Y.-C. Lin, G.A. Tompsett, G.W. Huber, J. Catal. 270 (2010) 110–124.
[16] A. Marcilla, M.I. Beltran, R. Navarro, Appl. Catal. B: Environ. 86 (2009) 78–86.
[17] M. Ibanez, M. Artetxe, G. Lopez, G. Elordi, J. Bilbao, M. Olazar, P. Castano, Appl. Catal. B: Environ. 148 (2014) 436–445.
[18] P. Castano, G. Elordi, M. Olazar, A.T. Aguayo, B. Pawelec, J. Bilbao, Appl. Catal. B: Environ. 104 (2011) 91–100.
[19] D.P. Serrano, J. Aguado, J.M. Escola, ACS Catal. 2 (2012) 1924–1941.
[20] D.P. Serrano, J. Aguado, J.M. Escola, J.M. Rodriguez, G. San Miguel, J. Anal. Appl. Pyrolysis 74 (2005) 370–378.
[21] J. Aguado, D.P. Serrano, J.L. Sotelo, R. Van Grieken, J.M. Escola, Ind. Eng. Chem. Res. 40 (2001) 5696–5704.
[22] C. Dorado, C.A. Mullen, A.A. Boateng, Appl. Catal. B: Environ. 162 (2015) 338–345.
[23] X. Li, H. Zhang, J. Li, L. Su, J. Zuo, S. Komarneni, Y. Wang, Appl. Catal. A: Gen. 455 (2013) 114–121.
[24] K. Wang, K.H. Kim, R.C. Brown, Green Chem. 16 (2014) 727–735.
[25] G. Elordi, M. Olazar, G. Lopez, P. Castano, J. Bilbao, Appl. Catal. B: Environ. 102 (2011) 224–231.
[26] N. Al-Yassir, M.N. Akhtar, S. Al-Khattaf, J. Porous Mater. 19 (2012) 943–960.
[27] N. Rane, M. Kersbulck, R.A. van Santen, E.J.M. Hensen, Micropor. Mesopor. Mater. 110 (2008) 279–291.
[28] H.J. Park, H.S. Heo, J.K. Jeon, J. Kim, R. Ryoo, K.E. Jeong, Y.K. Park, Appl. Catal. B: Environ. 95 (2010) 365–373.
[29] J. Jae, G.A. Tompsett, A.J. Foster, K.D. Hammond, S.M. Auerbach, R.F. Lobo, G.W. Huber, J. Catal. 279 (2011) 257–268.
[30] V.R. Choudhary, A.K. Kinage, C. Sivadinarayana, P. Devadas, S.D. Sansare, M. Guisnet, J. Catal. 158 (1996) 34–50.
[31] D.B. Lukyanov, N.S. Gnep, M.R. Guisnet, Ind. Eng. Chem. Res. 34 (1995) 516–523.
[32] M. Guisnet, N.S. Gnep, Appl. Catal. A: Gen. 146 (1996) 33–64.
[33] R. Fricke, H. Kosslick, G. Lischke, M. Richter, Chem. Rev. 100 (2000) 2303–2405.
[34] D.B. Lukyanov, N.S. Gnep, M.R. Guisnet, Ind. Eng. Chem. Res. 33 (1994) 223–234.
[35] D.B. Lukyanov, T. Vazhnova, Appl. Catal. A: Gen. 316 (2007) 61–67.
[36] V.R. Choudhary, D. Panjala, S. Banerjee, Appl. Catal. A: Gen. 231 (2002) 243–251.
[37] K.W. Bladh, Geochim. Cosmochim. Acta 53 (1989) 1482.
[38] Y.Q. Yu, X.Y. Li, L. Su, Y. Zhang, Y.J. Wang, H.Z. Zhang, Appl. Catal. A: Gen. 447 (2012) 115–123.
[39] A. Ausavasukhi, T. Sooknoi, D.E. Resasco, J. Catal. 268 (2009) 68–78.
[40] K.T. Leth, A.K. Rovik, M.S. Holm, M. Brorson, H.J. Jakobsen, J. Skibsted, C.H. Christensen, Appl. Catal. A: Gen. 348 (2008) 257–265.
[41] Y. Yu, Y. Zeng, J. Zuo, F. Ma, X. Yang, X. Zhang, Y. Wang, Bioresour. Technol. 134 (2013) 198–203.
[42] X.Y. Li, L. Su, Y.J. Wang, Y.Q. Yu, C.W. Wang, X.L. Li, Z.H. Wang, Front. Environ. Sci. Eng. 6 (2012) 295–303.
[43] C. Torri, M. Reinikainen, C. Lindfors, D. Fabbri, A. Oasmaa, E. Kuoppala, J. Anal. Appl. Pyrolysis 88 (2010) 7–13.
[44] G.D. Meitzner, E. Iglesia, J.E. Baumgartner, E.S. Huang, J. Catal. 140 (1993) 209–225.
[45] N. Al-Yassir, M.N. Akhtar, K. Ogunronbi, S. Al-Khattaf, J. Mol. Catal. A: Chem. 360 (2012) 1–15.
[46] I. Nowak, J. Quartararo, E.G. Derouane, J.C. Vedrine, Appl. Catal. A: Gen. 251 (2003) 107–120.
[47] A. Ausavasukhi, Y. Huang, A.T. To, T. Sooknoi, D.E. Resasco, J. Catal. 290 (2012) 90–100.
[48] J.W. Kim, S.H. Park, J. Jung, J.K. Jeon, C.H. Ko, K.E. Jeong, Y.K. Park, Bioresour. Technol. 136 (2013) 431–436.
[49] Y.-T. Cheng, J. Jae, J. Shi, W. Fan, G.W. Huber, Angew. Chem. Int. Ed. 51 (2012) 1387–1390.
[50] V.R. Choudhary, V.S. Nayak, T.V. Choudhary, Ind. Eng. Chem. Res. 36 (1997) 1812–1818.
[51] J. Li, X. Li, G. Zhou, W. Wang, C. Wang, S. Komarneni, Y. Wang, Appl. Catal. A: Gen. 470 (2014) 115–122.
[52] G. Zhou, J. Li, Y. Yu, X. Li, Y. Wang, W. Wang, S. Komarneni, Appl. Catal. A: Gen. 487 (2014) 45–53.
[53] H. Zhang, J. Nie, R. Xiao, B. Jin, C. Dong, G. Xiao, Energy Fuels 28 (2014) 1940–1947.
[54] C.L. Williams, C.-C. Chang, P. Do, N. Nikbin, S. Caratzoulas, D.G. Vlachos, R.F. Lobo, W. Fan, P.J. Dauenhauer, ACS Catal. 2 (2012) 935–939.
[55] N. Nikbin, P.T. Do, S. Caratzoulas, R.F. Lobo, P.J. Dauenhauer, D.G. Vlachos, J. Catal. 297 (2013) 35–43.